



The synthesis of SBA-Pr-3AP@Pd and its application as a highly dynamic, eco-friendly heterogeneous catalyst for Suzuki–Miyaura cross-coupling reaction

Fatemeh Mohajer¹ · Ghodsi Mohammadi Ziarani¹ · Alireza Badiel²

Received: 22 April 2020 / Accepted: 20 July 2020
© Springer Nature B.V. 2020

Abstract

The hexagonal mesoporous organic–inorganic hybrid as a new nanocatalyst was prepared by the treatment of SBA-15 with (3-chloropropyl)triethoxysilane, the 2,4,6-triamino pyrimidine ligand, and then PdCl₂ to obtain the SBA-15-propyl-triamino pyrimidine@Pd called as SBA-Pr-3AP@Pd, which was examined through Suzuki–Miyaura cross-coupling reaction by several aryl halides and phenylboronic acid under mild conditions in high yield.

Keywords Decorated mesoporous silica · Suzuki–Miyaura cross-coupling · Heterogeneous nanoporous catalyst · 2,4,6-Triamino pyrimidine ligand · SBA-Pr-3AP@Pd

Introduction

The application of the nanoreactor as the particular nanochemical compounds such as dendrimers [1], carbon nanotubes [2], zeolites [3], and mesoporous silica is highly valuable [4, 5]. Among the several nanoreactors, mesoporous silica compounds, mainly SBA-15, have been extensively considered due to the high surface spaces, highly well-arranged structure, mechanical constancy, thick walls, and inert environment for the immobilization of transition metal nanoparticles [6, 7].

Electronic supplementary material The online version of this article (<https://doi.org/10.1007/s11164-020-04218-4>) contains supplementary material, which is available to authorized users.

✉ Fatemeh Mohajer
f.mohajer@alzahra.ac.ir

✉ Ghodsi Mohammadi Ziarani
gmohammadi@alzahra.ac.ir

¹ Department of Chemistry, Faculty of Physics and Chemistry, University of Alzahra, Tehran, Iran

² School of Chemistry, College of Science, University of Tehran, Tehran, Iran

Jiang and co-workers reported the generation of the 2D metals, such as mesoporous compounds with many active sites, which act as catalysts. The mesoporous metallic Ir nanosheets have high electrocatalytic activity in the oxygen evolution reaction (OER) [8]. In another attempt, palladium-catalyzed decarbonylative Suzuki–Miyaura of amides applied in the synthesis of biaryls through the activation of the N–C(O) amide bond [9–11].

The application of several nanoporous metals such as Cu, Ru, Rh, Pd, Pt, and Au under different conditions through electrochemical deposition was extensively increased in different reactions [12, 13]. Application of the metal nanoparticles in catalysis, particularly in organic moieties, has received much attention [14, 15]. As a result, palladium nanoparticles (Pd NPs) have received much consideration [16]. In this study, Pd NPs sustained on the two-dimensional hexagonal structures of SBA-15 to avoid accumulation [17]. The mesoporous structure of SBA-15 is full of silanol groups; this hydrophilic structure decreased the transportation of hydrophobic compounds. However, hybrid porous scaffolds of SBA-15 with ligands containing organic groups afforded the hydrophobic and hydrothermally steady structures to apply in organic synthesis [18, 19].

Suzuki–Miyaura is a coupling reaction to produce the biaryl compounds in the presence of the different catalysts, including Pd [20]. There are numerous kinds of Pd-attached ligand-based SBA-15, which were reported for the synthesis of biaryl compounds [2, 21–23]. Cao and co-workers designated the combination of a Pd-diimine@SBA-15 catalyst for the Suzuki–Miyaura coupling by immobilizing Pd ions and diimine-functionalized SBA-15 mesoporous [24], then in another attempt Sarkar and co-workers organized an SBA-15 functionalized by thiol in the presence of the Pd catalyst for Suzuki–Miyaura coupling reaction [25]. Ghorbani-Vaghei et al. designated the synthesis of the SBA-15/AO/Pd(II) nanocatalyst by grafting of the amidoxime group on SBA-15 silica in the presence of the PdCl₂ [26].

Carbon–carbon (Csp²–Csp²) bond-creating cross-coupling reactions used to give symmetrical and unsymmetrical compounds, which were used in several one-pot methods [27]. Also, it is clear that the Suzuki–Miyaura coupling reaction of aryl halides with aryl boronic acids is a practical approach to the synthesis of biaryl structures [9–11, 28]. Since the Pd-based homogeneous catalysis caused problems in the separation of the expensive palladium catalyst from the produced compounds [29], immobilization of Pd catalyst solved this problem to respect the green environment [30]. Thus, in the subject of palladium chemistry, the study of useful and recyclable catalysts is an important issue.

Also, inexpensive and environmentally benign heterogeneous catalytic complexes are striking development, which is essential in this subject. The abundant efforts have been dedicated to the growth of efficient and selective catalyst to be applied in the Suzuki–Miyaura coupling reaction [31, 32]. In this study, the functionalized SBA-15 compound has been used as the most common supports, which was developed the surface and stability of the catalyst in the Suzuki–Miyaura coupling reaction [33].

Results and discussion

Synthesis of SBA-Pr-Cl

In this process, SBA-15 was prepared according to the literature [34].

Synthesis of SBA-Pr-3AP

The 2,4,6-triaminopyrimidine compound (0.25 g) was added to the dispersed SBA-Pr-Cl (1 g) in EtOH, and Et₃N refluxed for 24 h. The obtained white powder was filtered and washed with excess EtOH, to remove any residual organosilane by soxhlation method using EtOH as solvent over a 24 h to obtain SBA-Pr-3AP as the white powder, which was dried at ambient temperature.

Immobilization of Pd(II) ions on surface of SBA-Pr-3AP@Pd

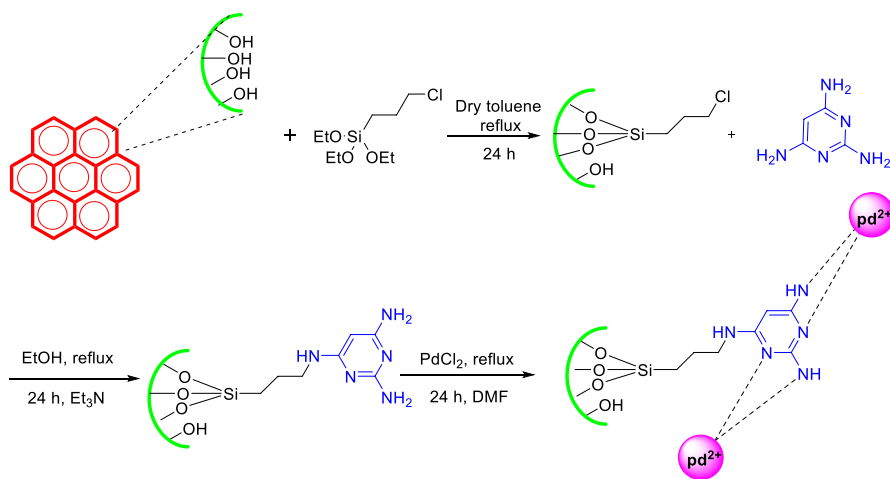
SBA-Pr-3AP (1.0 g) and palladium chloride (0.2 g) in EtOH (40 mL) was refluxed for 24 h. The dark gray powder as a resulting solid was filtered, washed with acetone, and dried in vacuum at 80 °C for 2 h to give SBA-Pr-3AP@Pd. According to the AAS, 25.91 wt % of palladium was precipitated on the synthesized catalyst. Also, there is no Pd in the reaction solution until the 7th run.

Suzuki–Miyaura cross-coupling reaction

The mixture of various aryl halides (1 mmol), phenylboronic acid (1.3 mmol) and K₂CO₃ (2 mmol) was stirred at the round-bottom flask in the presence of SBA-Pr-3AP@Pd catalyst (0.002 g) in H₂O: EtOH (4 mL) under an air atmosphere at 100 °C. The reaction progress was checked by thin-layer chromatography (TLC). At the end of the reaction, the SBA-Pr-3AP@Pd catalyst was filtered off, and the mixture was cooled down to ambient temperature. Next, the organic layer was extracted with chloroform and water. The resulting residue was purified by plate chromatography using *n*-hexane and ethyl acetate as eluents. The chemical structure of the desired products was confirmed by melting point and GC–MS analysis.

Characterization and synthesis of catalyst

In the first step, SBA-15 reacted with (3-chloropropyl)triethoxysilane in dry toluene under reflux condition to form SBA-Pr-Cl [35], which reacted with the 2,4,6-triamino pyrimidine in EtOH using Et₃N as a base under reflux condition to give SBA-Pr-3AP. In the last step, the Pd ions were immobilized on the nanoheterogeneous surface catalyst of SBA-Pr-3AP (Scheme 1), which was characterized by XRD, SEM, FT-IR, N₂ adsorption–desorption, EDX, and TGA analysis. The



Scheme 1 The synthetic procedure for the preparation of SBA-Pr-3AP@Pd catalyst

immobilized palladium catalyst was used in the Suzuki–Miyaura cross-coupling reaction as an efficient catalyst [36].

FT-IR analysis

To characterize and confirm the functionalized groups on the catalyst, FT-IR spectroscopy was applied, as shown in Fig. 1 for (a) SBA-15 (b) SBA-Pr-Cl, (c) SBA-Pr-3AP and (d) SBA-Pr-3AP@Pd. The bands at 800, 960, and 1100 cm^{-1} , are

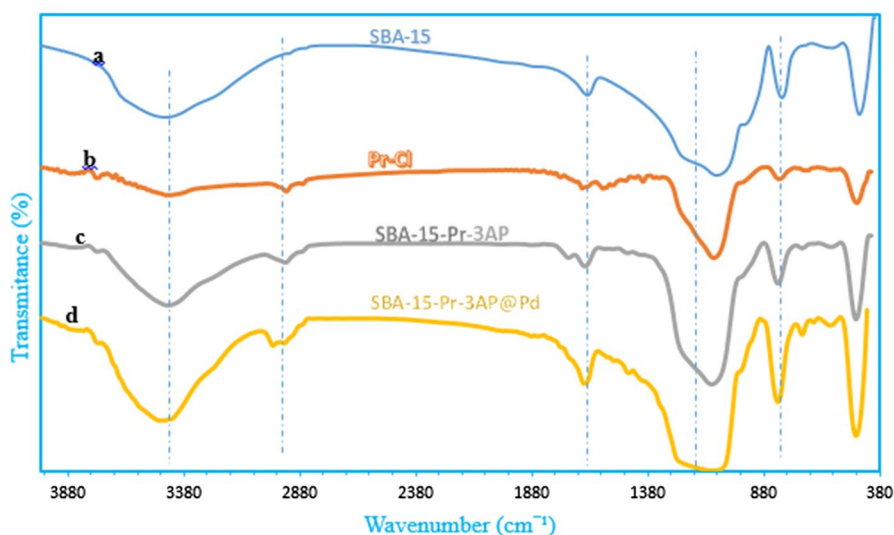


Fig. 1 FT-IR spectra of a SBA-15, b SBA-Pr-Cl c SBA-Pr-3AP d SBA-Pr-3AP@Pd

existing in all spectra, which are related to Si–O–Si symmetrical stretching vibrations, Si–OH symmetrical stretching vibrations, and unsymmetrical stretching vibrations of Si–O–Si spectroscopy, respectively. In the SBA-Pr-Cl (b), SBA-Pr-3AP (c), and SBA-Pr-3AP@Pd (d), the peaks appearing at 2852 and 2956 cm^{-1} are the representative of aliphatic CH_2 groups, which demonstrates the propyl group into the pore walls of SBA-15. The peak around 600–800 cm^{-1} shows Cl group in the second spectrum. The stretching vibration of the carbon–carbon double bond in aromatic ring appeared at 1554 cm^{-1} , and the peaks of 1454 cm^{-1} displayed stretching vibrations of the C=N group for the spectra of (c) and (d). The band at 1648 cm^{-1} is due to the imine bond of the aromatic ring and its stretching vibrations displayed at 705 cm^{-1} . Moreover, the band at 578 cm^{-1} in the spectrum of SBA-Pr-3AP@Pd is assigned to stretching of Pd–N [37]. These results showed that the synthesized SBA-15 was effectively functionalized with Pd species and obtained the final catalyst SBA-Pr-3AP@Pd.

EDX analysis

The EDX spectrum in Fig. 2 explains the presence of the elements C, N, O, Si, and Pd in SBA-Pr-3AP@Pd. The palladium peak displays the immobilization of the Pd nanoparticles on the surface of SBA-Pr-3AP@Pd.

BET analysis

The nitrogen adsorption–desorption isotherms and the BJH pore size distribution (based on the adsorption branch of the isotherms) for all samples SBA-15, SBA-Pr-3AP, and SBA-Pr-3AP@Pd are shown in Figs. 3 and 4. Type IV characterizes the isotherms with an H1-type hysteresis loop defined by IUPAC, demonstrating

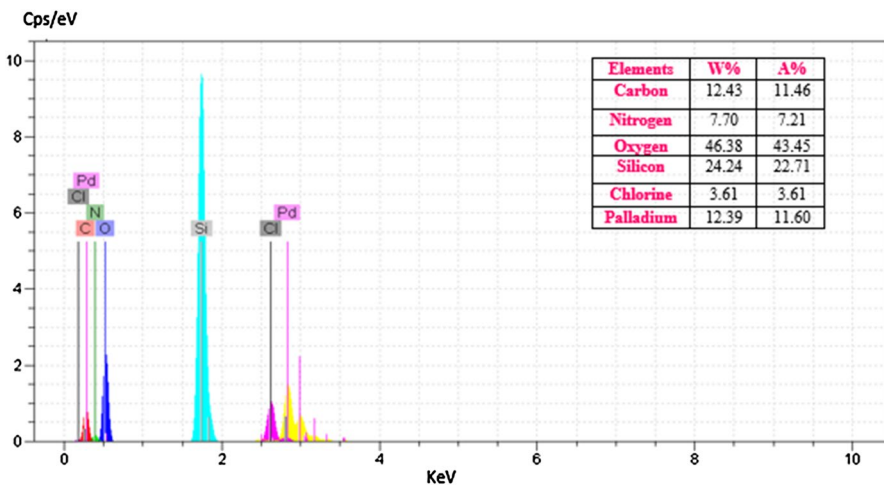


Fig. 2 EDX Spectrum of SBA-Pr-3AP@Pd

Fig. 3 N₂ adsorption–desorption isotherms of **a** SBA-15, **b** SBA-Pr-3AP, **c** SBA-Pr-3AP@Pd

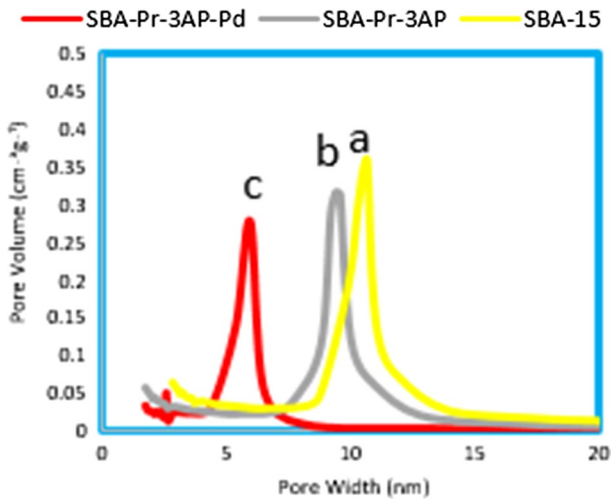
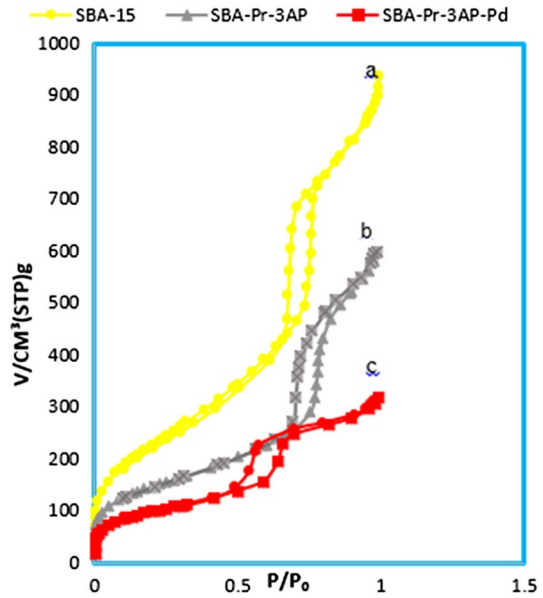


Fig. 4 BJH pore size distribution curves of **a** SBA-15, **b** SBA-Pr-3AP, **c** SBA-Pr-3AP@Pd

Table 1 Texture properties of **a** SBA-15, **b** SBA-Pr-Cl **c** SBA-Pr-3AP **d** SBA-Pr-3AP@Pd

| Entry | Catalyst | S_{BET}^a (m ² g ⁻¹) | V^a (cm ³ g ⁻¹) | D_{BJH}^a (nm) |
|-------|---------------|--|--|-------------------------|
| 1 | SBA-15 | 898 | 0.99 | 9.9 |
| 3 | SBA-Pr-3AP | 521 | 0.79 | 7.4 |
| 4 | SBA-Pr-3AP@Pd | 351 | 0.49 | 5.2 |

^a S_{BET} is a specific surface area, V total pore volume, and D_{BJH} average pore diameter

the well-ordered mesoporous arrangement of SBA-15. Table 1 presents the results for three structural parameters of the samples, including specific surface area (BET method), total pore volume, and pore diameter (BJH method). Successful incorporation of functional organic materials into mesoporous SBA-15 silica pores and the inclusion of Pd into this structure shifted the pore size to a smaller value and led to diminishing in pore volume and surface area.

XRD analysis

Low-angle XRD patterns of SBA-15 and SBA-Pr-3AP@Pd catalyst are shown in Fig. 5. SBA-15 has a strong diffraction reflection (100) and two small diffraction reflections (110) and (200) due to hexagonal symmetry and its long-range ordering structure [38]. The SBA-Pr-3AP@Pd marks a decrease in the overall intensity of the (100), (110), and (200), which might be related to the organic compounds and Pd-attached particles.

There is a flat pattern in the wide-angle XRD diffraction pattern, which is related to the pure SBA-15 and SBA-Pr-3AP. Two peaks around 40° and 45° could be attributed respectively to the (111) and (200), which are related to the metallic Pd(II), the fresh SBA-Pr-3AP@Pd catalyst diffractogram. It was proved that the Pd(II) was immobilized on the SBA-Pr-3AP (Fig. 6).

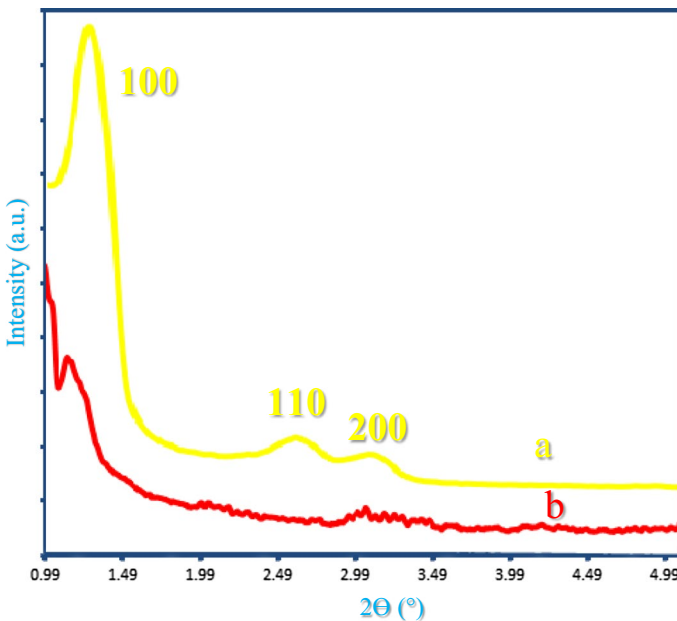


Fig. 5 Low-angle XRD patterns of a SBA-15, b SBA-Pr-3AP@Pd

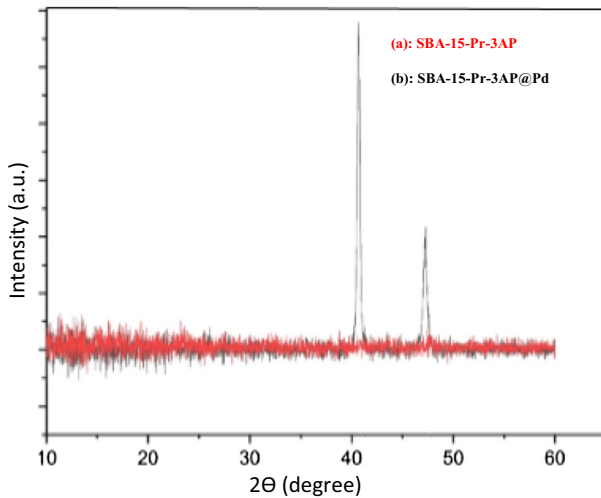


Fig. 6 The wide angle XRD patterns of **a** SBA-Pr-3AP, **b** SBA-Pr-3AP@Pd

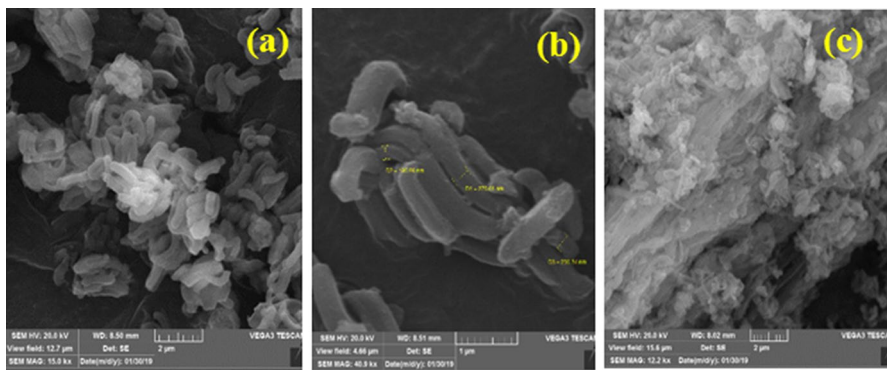


Fig. 7 SEM images of **a** SBA-Pr-Cl, **b** SBA-Pr-3AP, **c** SBA-Pr-3AP@Pd

SEM analysis

A typical scanning electronic microscopy (SEM) images of SBA-15 (a), SBA-Pr-3AP (b), and SBA-Pr-3AP@Pd (c) was not changed as shown in Fig. 7. In this case, the arrays of two-dimensional hexagonal mesoporous SBA-15 and the attachment of organic components inside the pore channels of SBA-15 silica has no distinct influence on the morphology of composition.

To approve the synthesized SBA-Pr-3AP@Pd catalyst nature, its TEM image was recorded after reaction completion, which showed the presence of Pd nanoparticles, as shown in Fig. 8.

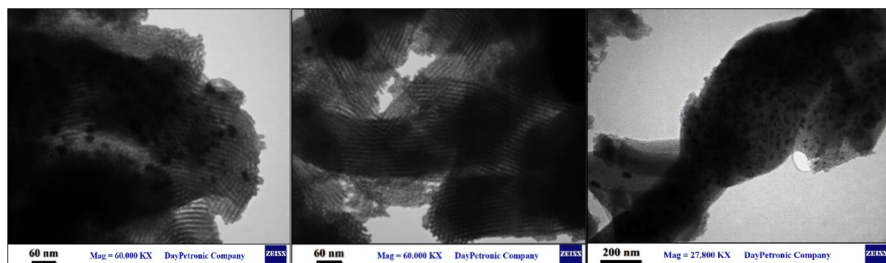


Fig. 8 TEM images SBA-Pr-3AP@Pd

TGA analysis

The thermal stability of the synthesized SBA was examined by thermogravimetric analysis. The TGA thermograms for the SBA-Pr-3AP and SBA-Pr-3AP@Pd displays the first weight loss below 200 °C, and this could be related to the desorption of physically adsorbed water (Fig. 9). The apparent mass change (18%) from 200 to 790 °C is probably due to the decomposition of organic groups. Moreover, relatively slow weight loss at elevated temperatures could be related to the dehydration of the surface –OH groups. So, the TGA curves confirm the successful grafting of organic groups onto the surface of silica.

The evaluation of the synthesized catalyst SBA-Pr-3AP@Pd was effected by its catalytic activities in the Suzuki–Miyaura cross-coupling reaction. Several parameters, such as solvent (EtOH, water, and toluene), the base quantity, and the catalyst amount, were optimized to find the best reaction conditions. The Suzuki–Miyaura coupling reaction model of 4-iodobenzene and phenylboronic acid under mild conditions with a little amount of Pd was designated as a typical reaction.

As shown in Table 2, the best result was obtained when the reaction was carried out in the presence of SBA-Pr-3AP@Pd in H₂O:EtOH as solvent using

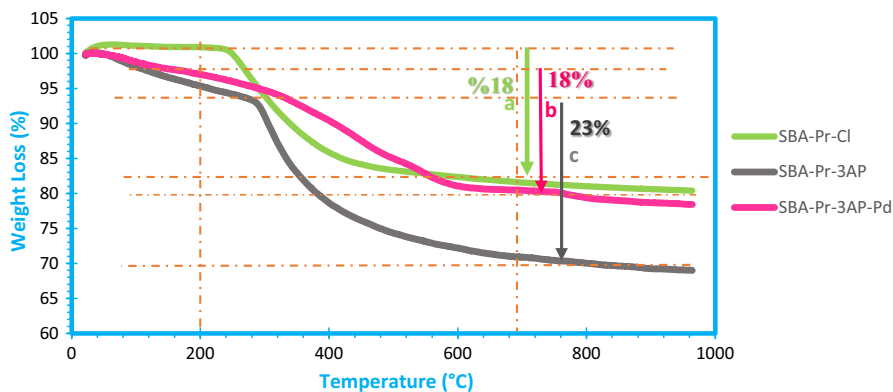
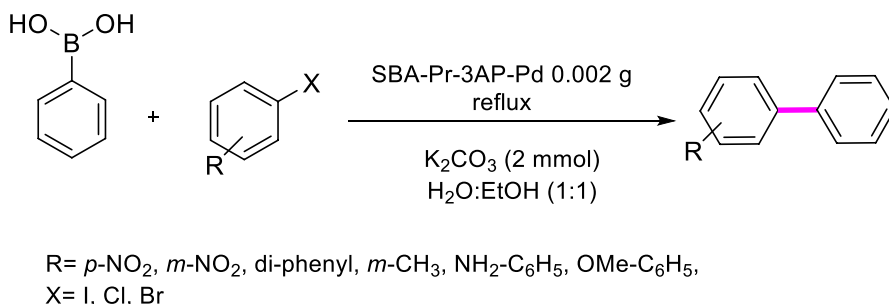


Fig. 9 TGA curves of a SBA-Pr-Cl, b SBA-Pr-3AP, c SBA-Pr-3AP@Pd

Table 2 Optimization of the reaction conditions

| Entry | Base | Solvent | Temp. (°C) | Pd (mol %) | Yield (%) ^b |
|-------|--------------------------------|-----------------------|------------|------------|------------------------|
| 1 | K ₂ CO ₃ | Toluene | 120 | 0.10 | 17 |
| 2 | K ₂ CO ₃ | DMF | 120 | 0.10 | 74 |
| 3 | K ₂ CO ₃ | DMSO | 120 | 0.10 | 71 |
| 5 | K ₂ CO ₃ | EtOH | 120 | 0.10 | 26 |
| 6 | K ₂ CO ₃ | Neat | 120 | 0.10 | Trace |
| 7 | – | DMF | 120 | 0.10 | – |
| 8 | Et ₃ N | DMF | 120 | 0.10 | 19 |
| 9 | NaOH | DMF | 120 | 0.10 | 80 |
| 10 | KOH | DMF | 120 | 0.10 | 83 |
| 11 | KOH | DMF | 110 | 0.10 | 91 |
| 12 | KOH | DMF | 100 | 0.10 | 93 |
| 13 | KOH | DMF | 90 | 0.10 | 92 |
| 14 | KOH | DMF | 100 | – | – |
| 15 | KOH | DMF | 100 | 0.05 | 96 |
| 16 | K ₂ CO ₃ | H ₂ O:EtOH | 120 | 0.002 | 96 |
| 17 | KOH | DMF | 100 | 0.07 | 96 |

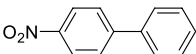
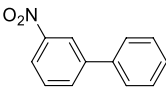
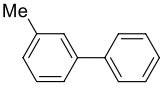
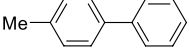
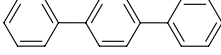
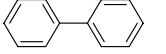
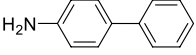
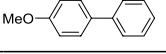
^aReaction conditions: 4-iodobenzene (1.0 mmol), phenylboronic acid (1.3 mmol), K₂CO₃ (2 mmol), SBA-Pr-3AP@Pd catalyst (0.002 g), base (2 mmol) and solvent (4 mL)

**Scheme 2** The Suzuki–Miyaura cross-coupling reaction in the presence of SBA-Pr-3AP@Pd catalyst

K₂CO₃ as a base at 100 °C. With the optimized conditions, the reaction was continued and completed (Scheme 2, Table 3). Various aromatic aryl halides with phenylboronic acid were reacted in the presence of the SBA-Pr-3AP@Pd as a catalyst and H₂O/EtOH as a solvent. It is important to mention that the time of the reaction in each of the products determined through TLC.

To display the value of this catalyst in the Suzuki–Miyaura reaction, the obtained results were compared with previously reported in the literature, as shown in Table 4, which was compared the reaction between phenylboronic acid and iodobenzene in the presence of different catalysts.

Table 3 The Suzuki–Miyaura cross-coupling reaction of various aryl phenylboronic acid and aryl halides in the presence of SBA-Pr-3AP@Pd catalyst^a

| Entry | X | R | Product | Time ^b (min) | Yield ^c (%) | mp (°C) [Refs.] |
|-------|-------------------|------|---|-------------------------|------------------------|-----------------|
| 1 | 4-NO ₂ | 1-Br |  | 40 | 94 | 111–114 [2] |
| 2 | 3-NO ₂ | 1-Br |  | 50 | 93 | 111–114 [19] |
| 3 | 4-Cl | 1-Br |  | 30 | 89 | 212 [2] |
| 4 | 3-Me | 1-Br |  | 40 | 94 | Oil [39] |
| 5 | 4-Me | 1-Br |  | 40 | 91 | 45–47 [40] |
| 6 | 4-Br | 1-Br |  | 50 | 100 | 212 [39] |
| 7 | H | I |  | 15 | 96 | 71–72 [21] |
| 8 | 4-NH ₂ | Br |  | 1 h | 92 | Oil [15] |
| 9 | 4-OMe | I |  | 40 | 89 | 89–91 [19] |

^aReaction conditions: ArX (1.0 mmol), phenylboronic acid (1.3 mmol), K₂CO₃ (2 mmol), SBA-Pr-3AP@Pd catalyst (0.002 g), and EtOH:H₂O (1:1) (4 mL)

^bTime of the reaction detected by TLC

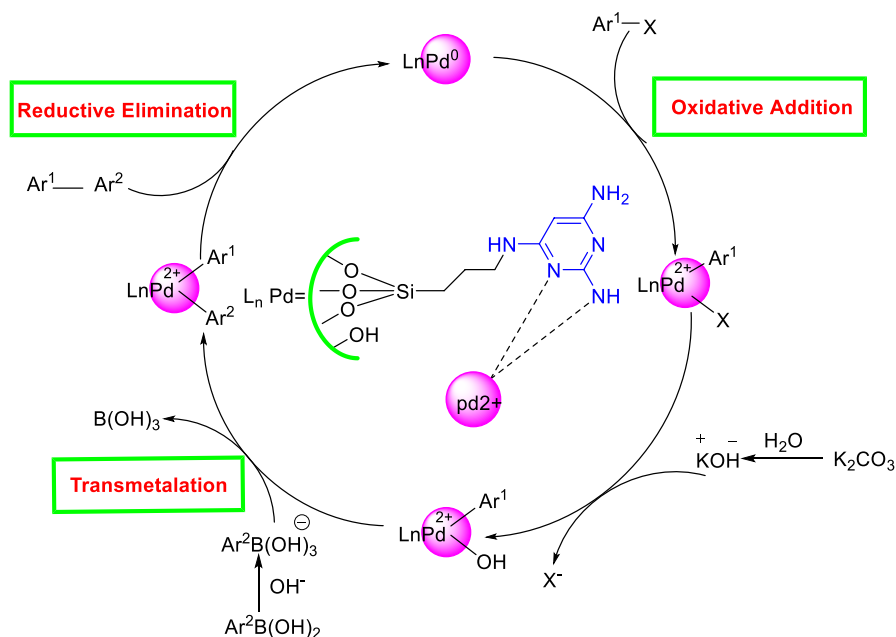
^cYield obtained by GC-MS

Table 4 A comparison of this work with some reported procedures

| No. | Catalyst | Temp. (°C) | Time (min) | Yield (%) |
|-----|--|------------|------------|--------------|
| 1 | Pd-SBA-16 | 70 | 4 h | 95 [41] |
| 2 | Pd(OAc) ₂ @SBA-15/PrNHEtNH ₂ | 80 | 20 | 97 [19] |
| 3 | SBA-15/AO/Pd(II) ^a | 50 | 18 | 98 [26] |
| 4 | SBA-15/di-urea/Pd | 70 | 20 | 99 [2] |
| 5 | SBA-Pr-3AP@Pd | 80 | 15 | 99 This work |

^aPd immobilized on amidoxime-functionalized Mesoporous SBA-15

The mechanism of the Suzuki–Miyaura cross-coupling reaction in the presence of SBA-Pr-3AP@Pd was illustrated in Scheme 3, which was described by the catalytic activity through three steps: oxidative addition, transmetalation, and reductive elimination [42]. In the oxidative addition step, aryl halides were added to Pd(0) complex to provide intermediate Ar–Pd(II)–X. In the second step, the



Scheme 3 Mechanism of the Suzuki–Miyaura cross-coupling reaction by SBA-Pr-3AP@Pd

aryl boronic acid was activated by a base which treated with aryl palladium (II) complex through the reductive elimination was afforded the desired product.

Catalyst leaching and recyclability

The catalyst leaching and recyclability were accomplished through the hot filtration test, to obtain the leaching of Pd from the catalyst during the reaction, for the Suzuki–Miyaura cross-coupling reaction under the optimal conditions was performed. In this process, after 10 min, the hot reaction mixture was filtered to separate the catalyst, and the reaction was continued under the supernatant solution. Through the GC–MS measurements, there is no increase in the product, and there is no Pd in the filtered solution by AAS (Atomic absorption spectrometry). So, this result proved that the Pd NPs were firmly grafted on the SBA-Pr-3AP@Pd duo to the excellent affinity between Pd NPs and 2,4,6-triamino pyrimidine ligand.

Reusability of catalyst

The recyclability of the heterogeneous catalysts is essential from the economic perspective. The method of reusing the SBA-Pr-3AP@Pd catalyst was manipulated for the Suzuki–Miyaura coupling reaction of 4-iodobenzene and phenylboronic acid upon optimized reaction conditions. After the accomplishment of each cycle, the solid catalyst was removed from the reaction easily, washed with ethyl acetate and

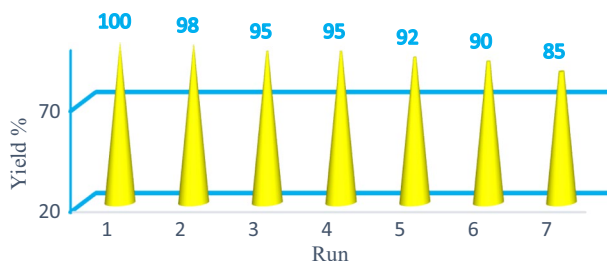


Fig. 10 Reusability study on the synthesis of the reaction of the 4-iodobenzene and phenylboronic acid

hot EtOH, after drying through vacuum overnight, then use again in a sequential run. The results in Fig. 10 determine that the supported catalyst was highly recyclable under the studied reaction conditions, preserving almost unaltered catalytic performance after seven uses.

To investigate the mechanism, the mercury drop test was used, as mercury amalgamated the heterogeneous catalyst in contrast with homogenous, [43] a drop of Hg(0) on the reaction texture of various reactant at reflux condition, no catalytic activity was pictured, which shows that Pd(0) and Pd(II) cycles [44–47].

Conclusion

In conclusion, Pd nanoparticles grafted in SBA-15 to afford active hybrid catalysts for applying in Suzuki–Miyaura cross-coupling reaction in aqueous media. The SBA-Pr-3AP@Pd catalyst could be simply removed and recovered from the reaction mixture. The catalytic activity did not decline even after reusing several times. The Suzuki–Miyaura coupling reaction was run through phenylboronic acid and various aryl halides under mild conditions with a little amount of Pd to obtain various diphenyl compounds. This catalyst afforded unique advantages such as excellent product yields, easy preparation, and short reaction times. Furthermore, the heterogeneous catalyst was easily recovered by filtration. The main point is that the hybrid catalyst used at least seven times without any problem. This catalyst could be proposed in other coupling reactions, such as Sonogashira or Heck.

Acknowledgements We are grateful for the Research Council support of Alzahra University.

Compliance with ethical standards

Conflicts of interest The authors declare that they have no conflict of interest.

References

1. C. Deraedt, L. Salmon, D. Astruc, *Adv. Synth. Catal.* **356**, 2525 (2014)
2. S. Rohani, G. Mohammadi Ziarani, A. Badiie, A. Ziarati, M. Jafari, A. Shayesteh, *Appl. Organomet. Chem.* **32**, e4397 (2018)
3. S. Lee, C. Jo, R. Ryoo, *J. Mater. Chem. A Mater.* **5**, 11086 (2017)

4. G. Mohammadi Ziarani, N. Lashgari, A. Badiei, *Curr. Org. Chem.* **21**, 674 (2017)
5. S.H. Petrosko, R. Johnson, H. White, C.A. Mirkin, *J. Am. Chem. Soc.* **138**, 7443 (2016)
6. M. Karimi, A. Badiei, G. Mohammadi Ziarani, *RSC Adv.* **5**, 36530 (2015)
7. G. Mohammadi Ziarani, P. Gholamzadeh, A. Badiei, V. Fathi Vavsari, *Res. Chem. Intermed.* **44**, 277 (2018)
8. B. Jiang, Y. Guo, J. Kim, A.E. Whitten, K. Wood, K. Kani, A.E. Rowan, J. Henzie, Y. Yamauchi, *J. Am. Chem. Soc.* **140**, 12434 (2018)
9. T. Zhou, C.-L. Ji, X. Hong, M. Szostak, *Chem. Sci.* **10**, 9865 (2019)
10. J. Buchspies, M. Szostak, *Catalysts* **9**, 53 (2019)
11. S. Shi, S.P. Nolan, M. Szostak, *Acc. Chem. Res.* **51**, 2589 (2018)
12. C. Li, M. Iqbal, B. Jiang, Z. Wang, J. Kim, A.K. Nanjundan, A.E. Whitten, K. Wood, Y. Yamauchi, *Chem. Sci.* **10**, 4054 (2019)
13. C. Li, H. Tan, J. Lin, X. Luo, S. Wang, J. You, Y.-M. Kang, Y. Bando, Y. Yamauchi, J. Kim, *Nano Today* **21**, 91 (2018)
14. D. Astruc, F. Lu, J.R. Aranzaes, *Angew. Chem.* **44**, 7852 (2005)
15. L.A. Bivona, F. Giacalone, L. Vaccaro, C. Aprile, M. Gruttadauria, *Chem. Cat. Chem.* **7**, 2526 (2015)
16. C. Yang, H. Wustefeld, M. Kalwei, F. Schiith, *Studies in Surface Science and Catalysis* (Elsevier, Amsterdam, 2004), p. 2574
17. G. Mohammadi Ziarani, S. Rohani, A. Ziarati, A. Badiei, *RSC Adv.* **8**, 41048 (2018)
18. D. Zhao, P. Yang, N. Melosh, J. Feng, B.F. Chmelka, G.D. Stucky, *Adv. Mater.* **10**, 1380 (1998)
19. S. Rostamnia, H. Xin, *Appl. Organomet. Chem.* **27**, 348 (2013)
20. N. Miyaura, A. Suzuki, *Chem. Rev.* **95**, 2457 (1995)
21. B. Abbas Khakiani, K. Pourshamsian, H. Veisi, *Appl. Organomet. Chem.* **29**, 259 (2015)
22. H. Veisi, M. Pirhayati, A. Kakanejadifard, *Tetrahedron Lett.* **58**, 4269 (2017)
23. N. Aayasha, S.M. Prachi, D. Negi, *Int. J. Sci. Basic Appl. Res.* **9**, 491 (2019)
24. J. Yu, A. Shen, Y. Cao, G. Lu, *Catalysts* **6**, 181 (2016)
25. S.M. Sarkar, M.L. Rahman, M.M. Yusoff, *New J. Chem.* **39**, 3564 (2015)
26. R. Ghorbani-Vaghei, S. Hemmati, H. Veisi, *J. Mol. Catal. A. Chem.* **393**, 240 (2014)
27. B. Cornils, W.A. Herrmann, M. Beller, R. Paciello, *Applied Homogeneous Catalysis with Organometallic Compounds: A Comprehensive Handbook in Four Volumes* (Wiley, Hoboken, 2017)
28. A. Suzuki, *J. Organomet. Chem.* **576**, 147 (1999)
29. R. Martin, S.L. Buchwald, *Acc. Chem. Res.* **41**, 1461 (2008)
30. S. MacQuarrie, B. Nohair, J.H. Horton, S. Kaliaguine, C. Crudden, *J. Phys. Chem. C* **114**, 57 (2009)
31. D.H. Lee, M. Choi, B.W. Yu, R. Ryoo, A. Taher, S. Hossain, M. Jin, *Adv. Synth. Catal.* **351**, 2912 (2009)
32. Y. Jiang, Q. Gao, *J. Am. Chem. Soc.* **128**, 716 (2006)
33. A. Corma, *Chem. Rev.* **97**, 2373 (1997)
34. D. Zhao, J. Feng, Q. Huo, N. Melosh, G.H. Fredrickson, B.F. Chmelka, G.D. Stucky, *Science* **279**, 548 (1998)
35. S. Rostamnia, E. Doustkhah, *RSC Adv.* **4**, 28238 (2014)
36. L.K. Mannepalli, C. Gadipelly, G. Deshmukh, P. Likhar, S. Pottabathula, *Bull. Chem. Soc. Jpn.* **93**, 355 (2020)
37. K. Mukhopadhyay, B.R. Sarkar, R.V. Chaudhari, *J. Am. Chem. Soc.* **124**, 9692 (2002)
38. G. Mohammadi Ziarani, N. Hosseini Mohtasham, N. Lashgari, A. Badiei, *Res. Chem. Intermed.* **41**, 7581 (2015)
39. V. Fathi Vavsari, G. Mohammadi Ziarani, S. Balalaie, A. Badiei, F. Golmohammadi, S. Ramezanpour, F. Rominger, *ChemistrySelect* **2**, 3496 (2017)
40. E. Doustkhah, S. Rostamnia, H.G. Hossieni, R. Luque, *ChemistrySelect* **2**, 329 (2017)
41. M. Niakan, Z. Asadi, M. Masteri-Farahani, *ChemistrySelect* **4**, 1766 (2019)
42. K. Matos, J.A. Soderquist, *J. Org. Chem.* **63**, 461 (1998)
43. D.E. Bergbreiter, P.L. Osburn, J.D. Frels, *Adv. Synth. Catal.* **347**, 172 (2005)
44. L. Wu, Y. Long, J. Ma, G. Lu, *Res. Chem. Intermed.* **45**, 3809 (2019)
45. J. Zhang, J. Chen, Q. Zhang, R. Wang, S. Wu, *Res. Chem. Intermed.* **45**, 2503 (2019)
46. H. Ünver, *Res. Chem. Intermed.* **44**, 7835 (2018)
47. E. Rafiee, M. Kahrizi, M. Joshaghani, P.G.S. Abadi, *Res. Chem. Intermed.* **42**, 5573 (2016)